Electronic Supplementary Material (ESI) for Inorganic Chemistry Frontiers.

Supporting Information

Proton-induced Switching of Excitation-Wavelength-Dependent Emission Based on Mixed-Ligand Metal-Organic Frameworks

Yuanchao Lv[a]‡, Xue Yang[a]‡, Zhile Xiong[a], Yunbin Li[a], Jiashuai Liang[a], Shengchang Xiang[a], and Zhangjing Zhang*[a]*

[a] *Fujian Provincial Key Laboratory of Polymer Materials, College of Chemistry and Materials Science, Fujian Normal University, Fuzhou 350007, China*

E-mail: lvyc@fjnu.edu.cn; zzhang@fjnu.edu.cn

Contents

Materials and experimental details

1. Materials

4,4′-(benzo [1,2,5]-thiadiazole-4,7-diyl) dibenzoic acid (H_2BTDB) and 4,4'-(benzo[c][1,2,5] thiadiazole-4,7-diyl)bis(3-aminobenzoic acid) (H_2BTAB) were synthesized through the classical Suzuki condensation reaction[1]. 4,7-Dibromo-2,1,3-Benzothiadiazole, Methyl 4-Boronobenzoate Methyl 3-amino-4-bromobenzoate, $PdCl_2$ (dppf), KOH, K_2CO_3, 4,7-Bis(4,4,5,5-tetramethyl-1,3,2-dioxaborolan-2-yl)-2,1,3-benzothiadiazole and $SrCl_2$ were purchased from Aldrich Chemical Co. and used without further purification. Organic solvents, CH_2Cl_2, 1,4-dioxane, DMF, were dried and distilled before use.

2. Synthesis of the **FJU-221** and ML-MOFs (**ML-MOF-1** to **ML-MOF-8**) crystals.

Synthesis of **FJU-221**: A mixture of $SrCl_2$ (3 mg, 0.019 mmol), H_2BTDB (2 mg, 0.14 mmol), 1.5 ml of DMF and 0.5 mL of H_2O was stirred for 5 min and then transferred into a 10 mL vessel. After maintaining the mixture at 100 ℃ for 24 h, the reaction system was slowly cooled to room temperature. The resulting yellow transparent block-like crystals were collected after being washed with DMF and deionised water several times to rid them of excess metals and ligands. While, pure-BTAB-based MOF can not be obtained possibly due to the faster molecular aggregation of BTAB rather than the growth of regular crystals of BTAB.

Synthesis of **ML-MOFs-1** to **ML-MOF-8**: A mixture of $SrCl_2$ (3 mg, 0.019 mmol), H_2BTDB (2 mg, 0.14 mmol), different molar content of H_2BTAB (5 %, 10 %, 15 %, 20 %, 25 %, 30 %, 35 %, 40 % of the molar quantity of H_2BTDB, respectively), 1.5 ml of DMF and 0.5 mL of H_2O was stirred for 5 min and then transferred into a 10 mL vessel. After maintaining the mixture at 100 ℃ for 24 h, the reaction system was slowly cooled to room temperature. The resulting yellow or orange red transparent block-like crystals were collected after being washed with DMF and deionised water several times to rid them of excess metals and ligands.

3. Characterizations

X-ray diffraction (XRD, Japan Rigaku D/max-2500) was measured with Cu Kα radiation. Infrared spectra were obtained on PerkinElmer Spectrum Two FT-IR Spectrometer. Thermogravimetry analysis (TGA) of the compounds was conducted on a SHIMADZU TGAQ50 thermogravimetric analyzer from room temperature to 600 ℃ at a heating rate of 10 ℃/min under N_2 atmosphere. The absolute quantum yields were measured by using a steady and transient fluorescent spectrometer (Edinburgh instruments, FLS980). The fluorescence decay measurement was performed on a Quantaurus-Tau compact fluorescence lifetime spectrometer (Hamamatsu photonics, C11367-31). The fluorescence spectra were measured on a UV-visible spectrometer (Perkin-Elmer Lambda 35) and a fluorescent spectrometer

(Hitachi F-7000), respectively. Bright-field optical images and fluorescence microscopy images were taken from an inverted fluorescence microscope (Nikon Ti-U), by exciting the samples with a mercury lamp.

Figure S1. The schematic diagram illustrating the strategy to tune the emission properties of D-A-D type organic linkers by changing the donor group.

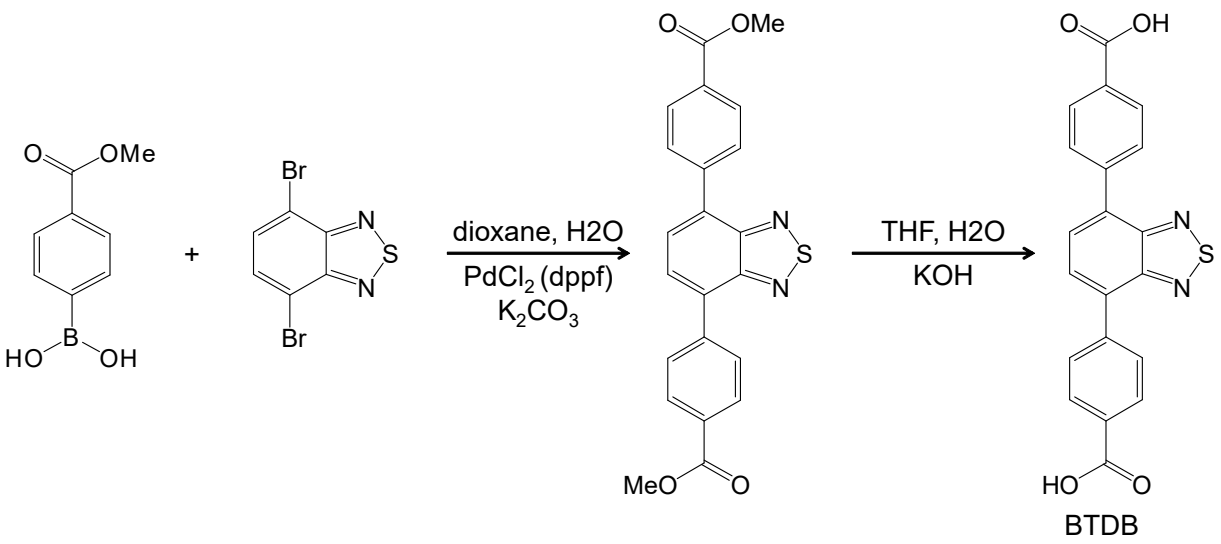

Figure S2. Synthetic route of BTDB molecule.

Step 1: The synthesis of dimethyl 4,4′-(benzo[c][1,2,5]-thiadiazole-4,7-diyl) dibenzoate.

4,7-Dibromo-2,1,3-Benzothiadiazole (1 g, 3.4 mmol), Methyl 4-boronobenzoate (1.4 g, 7.8 mmol), PdCl2(dppf) (0.17 mmol, 124 mg) and K_2CO_3 (16 mmol, 2.2 g) were added in a solution containing 75 mL dioxane and 15 mL water. The reaction solution was degassed three times. Then the mixture was heated to reflux at 100 ℃ for 24 h under nitrogen atmosphere. After cooling down to room temperature, the mixture was filtrated. DI water was added to the filtrate to get the solid product. The crude product was obtained after filtration and washed using DI water, which was directly used for next step without further purification (orange-red solid, 1.1 g, 80.1 %).

Step 2: The synthesis of 4,4′- (benzo[c][1,2,5]-thiadiazole-4,7-diyl) dibenzoic acid (BTDB)

dimethyl 4,4′-(benzo[c][1,2,5]-thiadiazole-4,7-diyl) dibenzoate (2.5 mmol, 1 g) was added to a solution containing 100 mL THF and 25 mL water with 2 g KOH. The mixture solution was heated to reflux at 80 °C overnight. After cooling down to room temperature, the mixture was filtrated. Then the filtrate was neutralized using 6M HCl to obtain the precipitate, which was filtered to offer the final product 4,4′-(benzo[c][1,2,5]-thiadiazole-4,7-diyl) dibenzoic acid (BTDB) as a green solid (0.8 g, 86 %). 1H NMR: (400 MHz, DMSO-d6) δ ppm 8.14 (8H) 8.08 (2H).

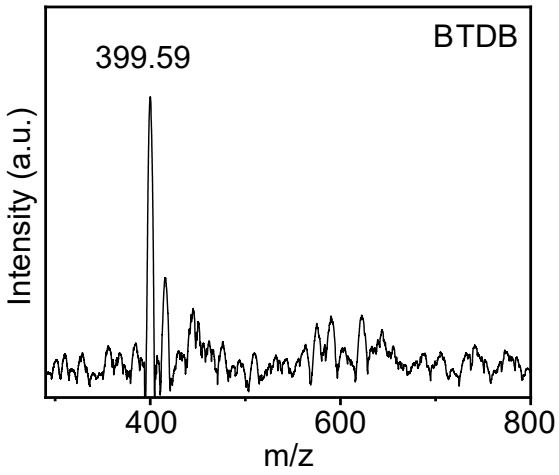

Figure S3. Mass spectrum of BTDB.

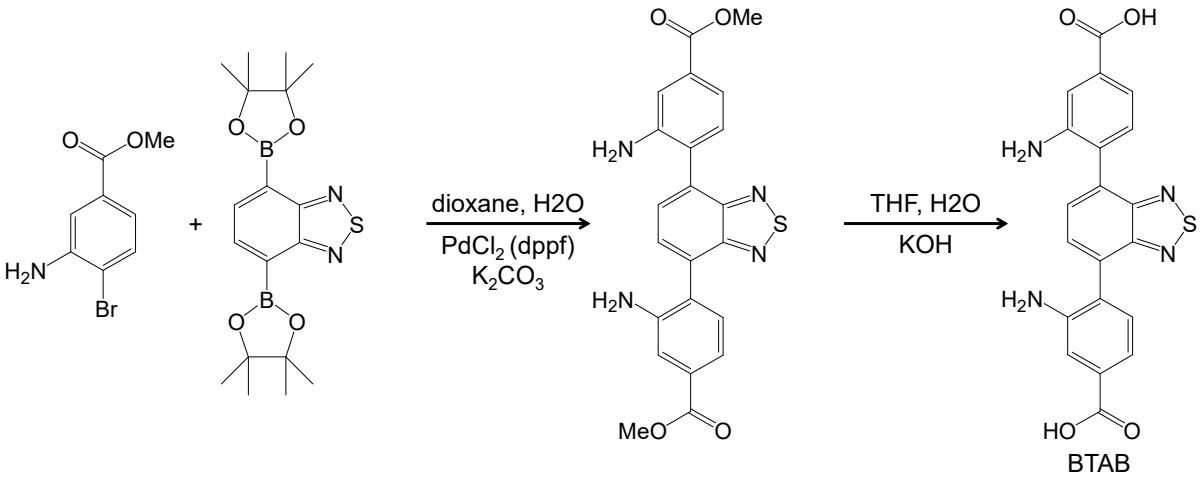

Figure S4. Synthetic route of BTAB molecule

Step 1: The synthesis of dimethyl 4,4'-(benzo[c][1,2,5]thiadiazole-4,7-diyl)bis(3-aminobenzoate).

Methyl-3-amino-4-bromobenzoate (6.1 mmol, 1.4 g), 4,7-Bis(4,4,5,5-tetramethyl-1,3,2-dioxaborolan-2-yl)-2,1,3-benzothiadiazole (2.6 mmol, 1 g), $PdCl_2$(dppf) (0.12 mmol, 90 mg) and K_2CO_3 (16 mmol, 2.2 g) were added in a solution containing 75 mL dioxane and 15 mL water. The reaction solution was degassed three times. Then the mixture was heated to reflux at 100 ℃ for 24 h under nitrogen atmosphere. After cooling down to room temperature, the mixture was filtrated. DI water was added to the filtrate to get the solid product. The crude product was obtained after filtration and washed using DI water, which was directly used for next step without further purification (orange-red solid, 0.9 g, 80.4 %).

Step 2: The synthesis of 4,4'-(benzo[c][1,2,5]thiadiazole-4,7-diyl)bis(3-aminobenzoic acid) (BTAB)

Dimethyl 4,4'-(benzo[c][1,2,5]thiadiazole-4,7-diyl)bis(3-aminobenzoate) (2.0 mmol, 1 g) was added to a solution containing 100 mL THF and 25 mL water with 2 g KOH. The mixture solution was heated to reflux at 80 °C overnight. After cooling down to room temperature, the mixture was filtrated. Then the filtrate was neutralized using 6M HCl to obtain the precipitate, which was filtered to offer the final product 4,4'-(benzo[c][1,2,5thiadiazole-4,7-diyl)bis(3-aminobenzoic acid) (BTAB) as a brown solid (0.8 g, 85.1 %). 1H NMR (400 MHz, DMSO-d6) δ ppm 7.66 (2H) 7.38 (2H), 7.21 (2H), 7.10 (2H).

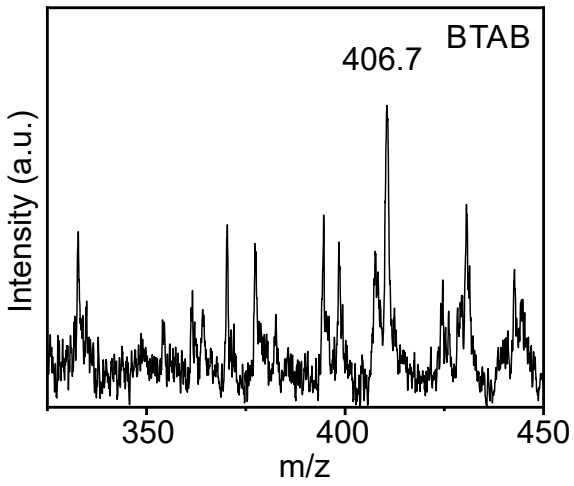

Figure S5. Mass spectrum of BTAB.

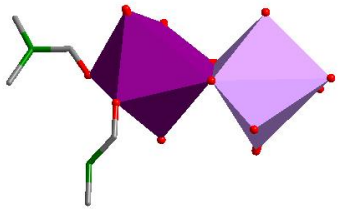

Figure S6. SBU of **FJU-221**

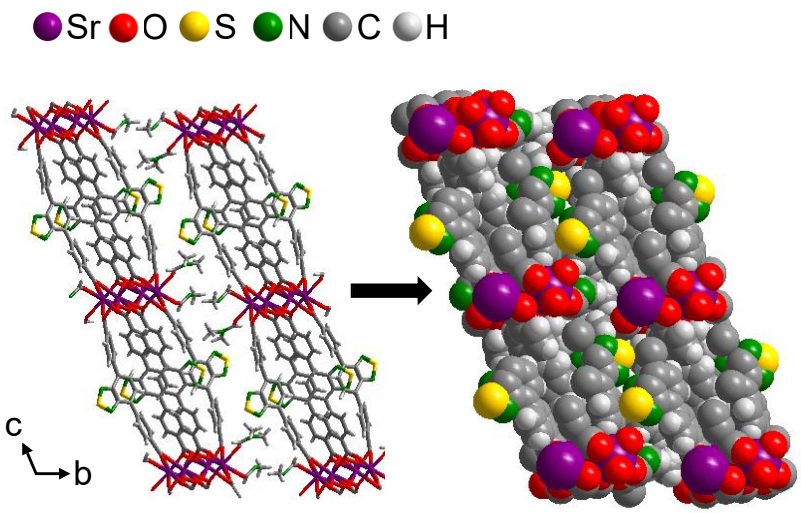

Figure S7. Sphere packing struture for **FJU-221**.

The obtained sphere packing in Figure S7 showed a close-packing structure. The void ratio data of 8.5 % should be attributed to the spaces between ligands or layers.

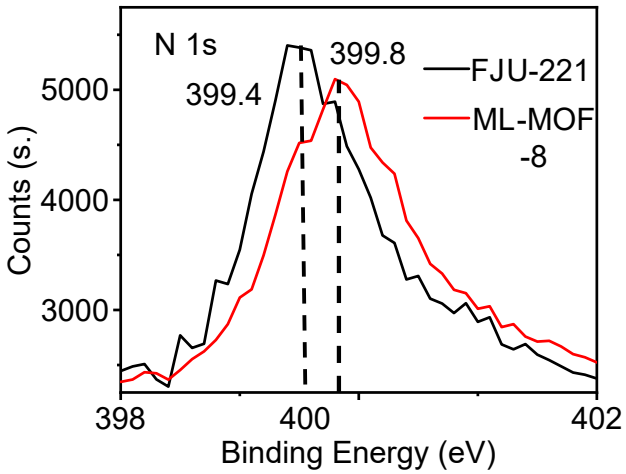

Figure S8. XPS spectra of **FJU-221** and **ML-MOF-8** at binding energy to N 1s.

The XPS spectra of **FJU-221** and **ML-MOF-8** at binding energy to N 1s were acquired. In the Figure S8, the N 1s binding energy of **ML-MOF-8** move to a higher value, which reveal that the introduction of N from amino group, confirming the existence of BTAB ligand.

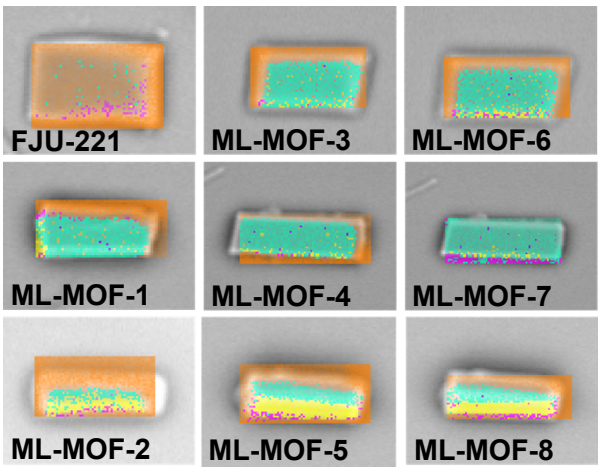

Name	N (%)
FJU-221	10.56
ML-MOF-1	11.10
ML-MOF-2	11.50
ML-MOF-3	12.10
ML-MOF-4	12.57
ML-MOF-5	12.78
ML-MOF-6	12.92
ML-MOF-7	13.43
ML-MOF-8	14.32

Figure S9. SEM-EDX images and N percentage of **FJU-221** and ML-MOFs (**ML-MOF-1** to **ML-MOF-8**).

The SEM-EDX elemental mapping data of **FJU-221** and ML-MOFs were collected as shown in Figure S9, with increasing the BTAB content, the N percentage increased gradually from 10.56 % to 14.32 % due to the introduction of amino group from BTAB, confirming the successful doping of BTAB by adding BTAB into the mother liquor.

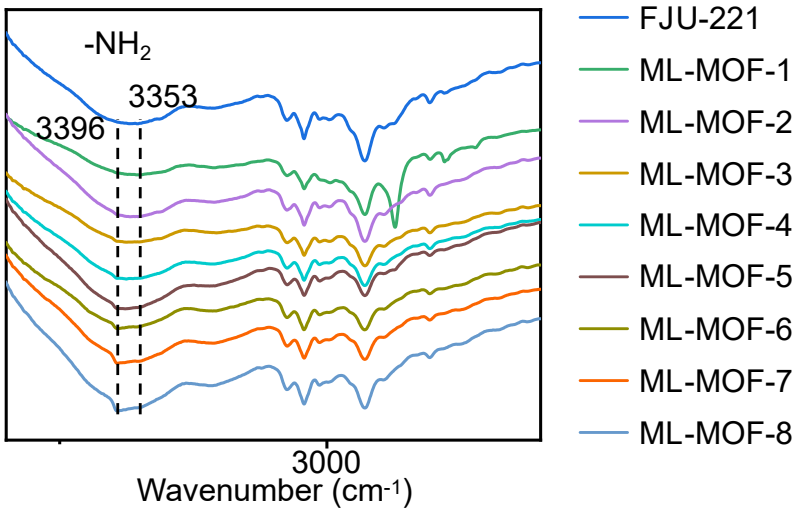

Figure S10 FTIR spectra of **FJU-221** and **ML-MOF-1** to **ML-MOF-8**.

We further collected the FTIR spectra including **FJU-221** and **ML-MOF-1** to **ML-MOF-8**. In Figure S10, the characteristic peak 3300-3400 cm^{-1} attributed to amino group exhibited strengthening trend with the increase of BTAB, further confirming the successful doping of BTAB.

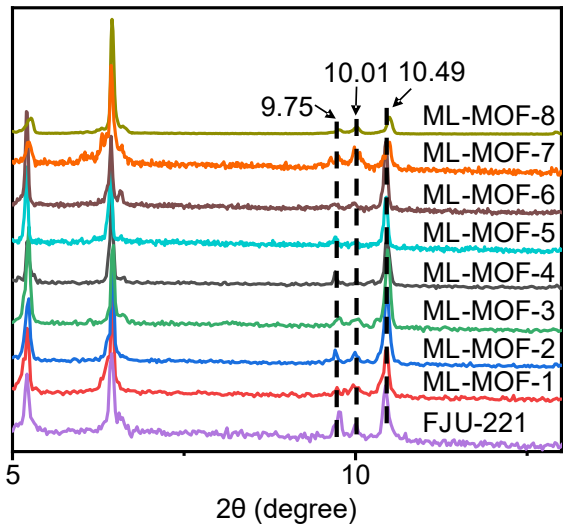

Figure S11. Amplified PXRD patterns of as-synthesized crystals: **FJU-221**, **ML-MOF-1**, **ML-MOF-2**, **ML-MOF-3**, **ML-MOF-4**, **ML-MOF-5**, **ML-MOF-6**, **ML-MOF-7**, and **ML-MOF-8**.

The PXRD patterns of all these ML-MOFs at 9.75, 10.01 and 10.49 degree are almost identical to that of the **FJU-221**, confirming their isostructural nature and high phase purity. We also found that, with the increase of the BTAB content, the ML-MOFs patterns exhibit the subtle difference on diffraction intensity, which may be attributed to incomplete exposure of crystal surface during the data collection.

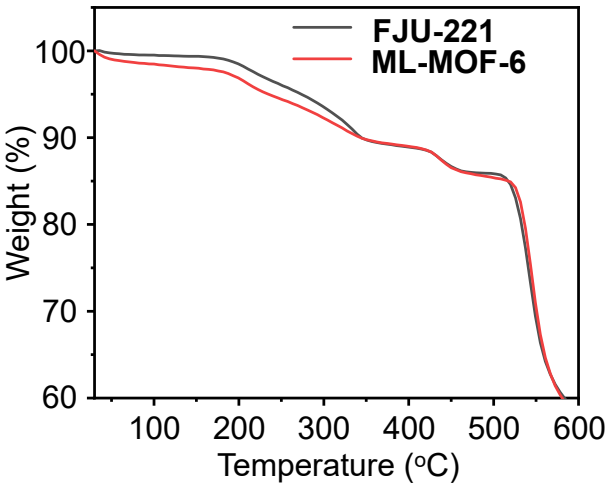

Figure S12. Thermogravimetric analysis (TGA) of **FJU-221** and **ML-MOF-6**.

Thermogravimetric analysis (TGA) for the **FJU-221** and **ML-MOF-6** shows a continuous weight loss of 15 % from 170 ℃ due to the coordinating DMF moleculars.

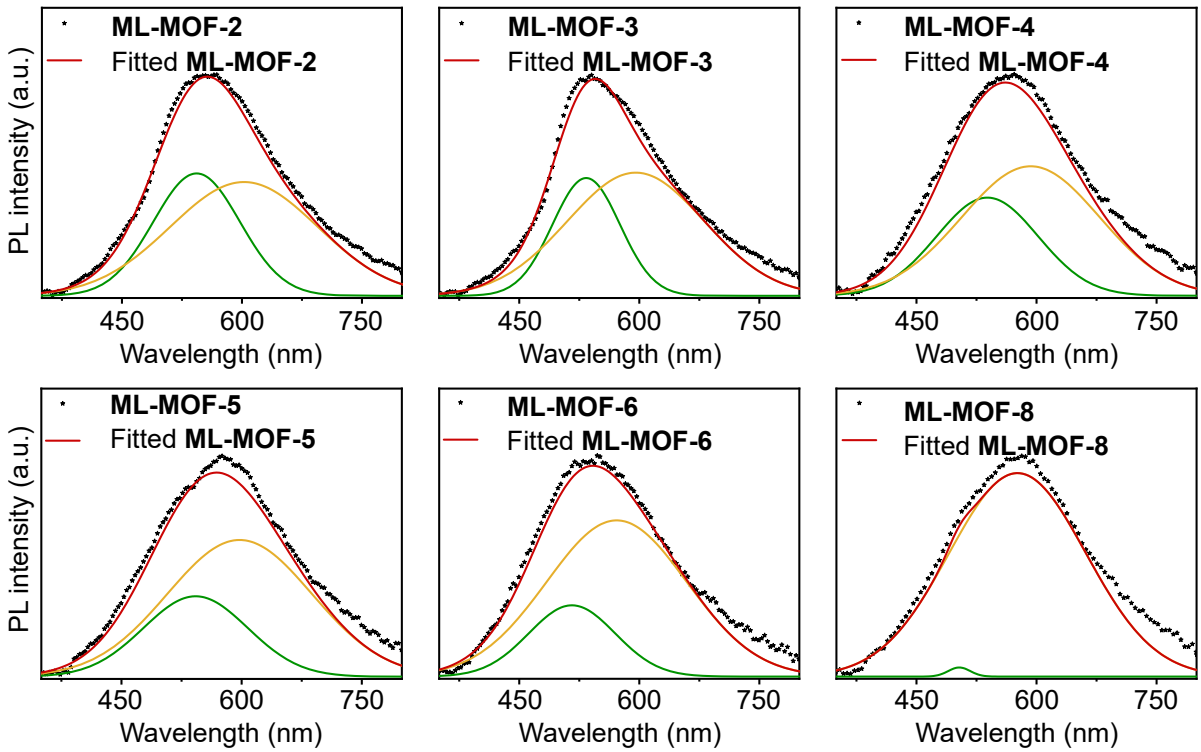

Figure S13. PL spectra of **ML-MOF-2 to ML-MOF-6,** and **ML-MOF-8** at 295 nm excitation

The emission of these ML-MOFs can be divided into two peaks, including 520 nm for the emission of BTDB and 580 nm for the ET emission. The asterisk is the original emission spectrum, and the red line is the fitted emission curve.

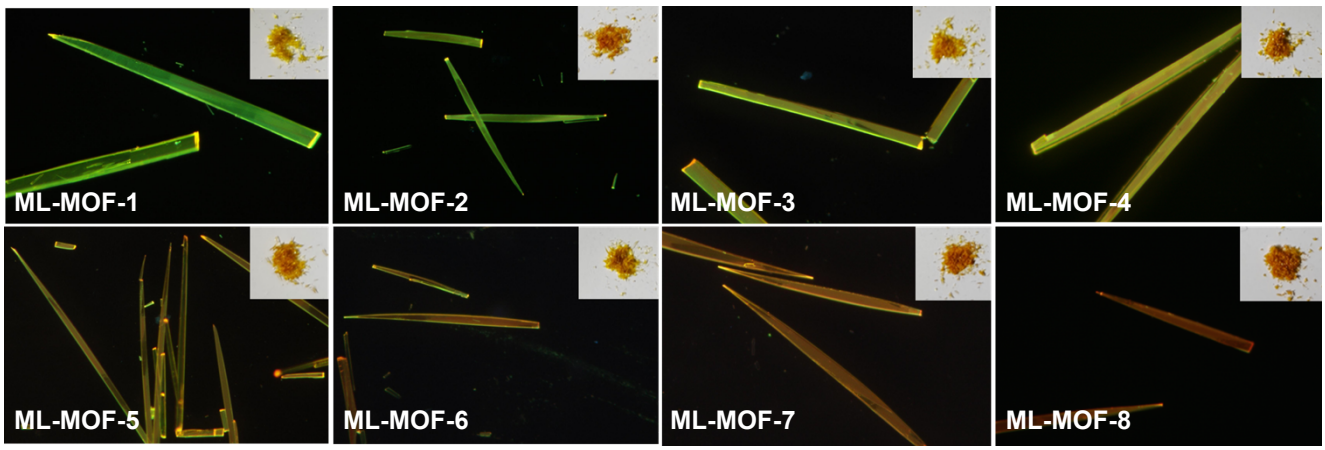

Figure S14. PL images of **ML-MOF-1** to **ML-MOF-8** under 295 nm UV lamp.

By increasing the molar content of BTAB, these ML-MOFs exhibit tunable color from green to orange-red under the excitation of 295 nm. And the crystal appearance color also gradually deepened from yellow to orange under the light.

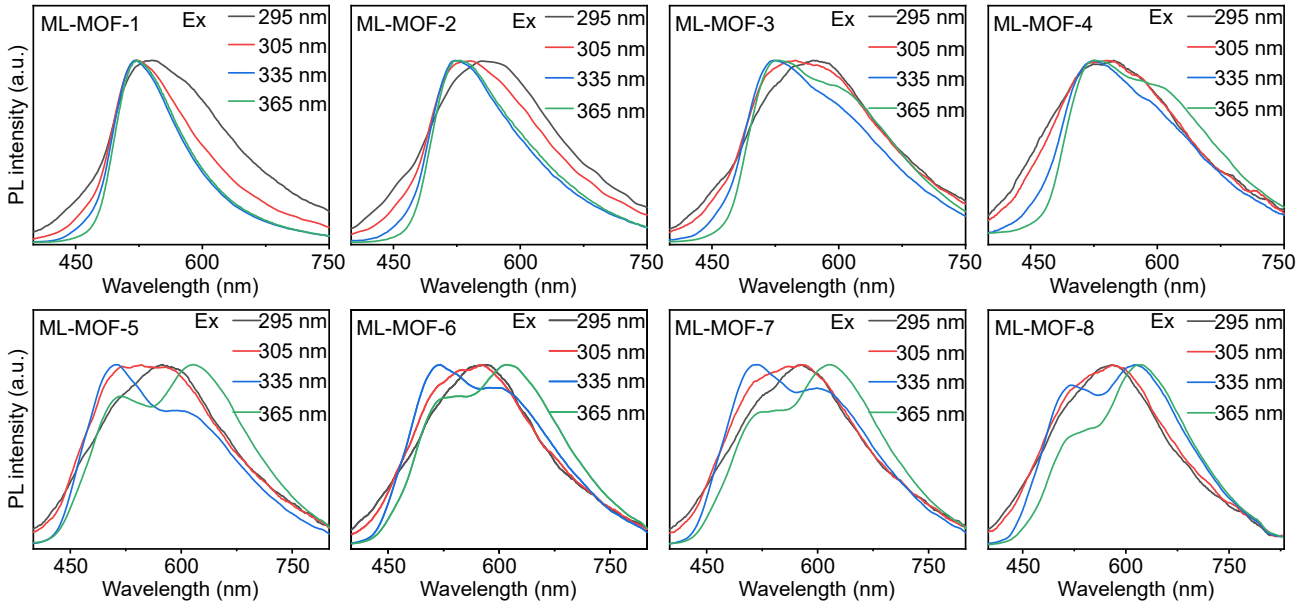

Figure S15. PL spectra of the **ML-MOFs** (**ML-MOF-1** to **ML-MOF-8**) under the excitation of 295 nm, 305 nm, 335 nm and 365 nm.

The the emission peaks of the **ML-MOFs** (**ML-MOF-3** to **ML-MOF-8**) changed from the single emission to the dual emission with the excitation wavelength increasing from 295 to 365 nm.

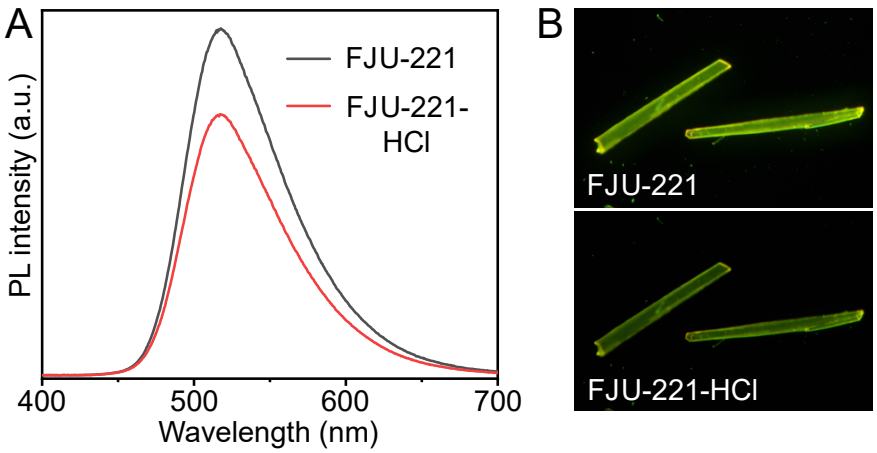

Figure S16. (A) PL spectra of **FJU-221** and **FJU-221-HCl**. (B) PL images of **FJU-221** and **FJU-221-HCl**.

Under HCl fuming, the PL intensity of **FJU-221** decreased a little, which may be due to the damage to framework structure during HCl treatment and thus lead to a slight reduction in emission intensity. But the **FJU-221** still kept the green emission, which ruled out the protonation process on the **FJU-221**. Therefore, in this work, the protonation in ML-MOFs should be attributed to the amino group from BTAB rather than the N atoms on benzothiadiazole.

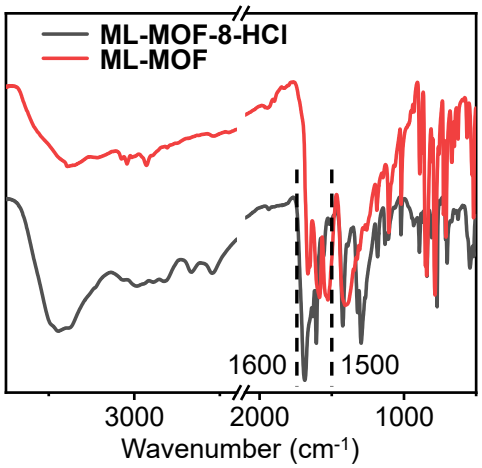

Figure S17. Infrared spectra of **ML-MOF-8** and **ML-MOF-8-HCl**.

The full FTIR spectra of the initial **ML-MOF-8** and **ML-MOF-8-HCl** are compared. The change in the band (1600-1500 cm^{-1}) confirms the protonation of the amino group.

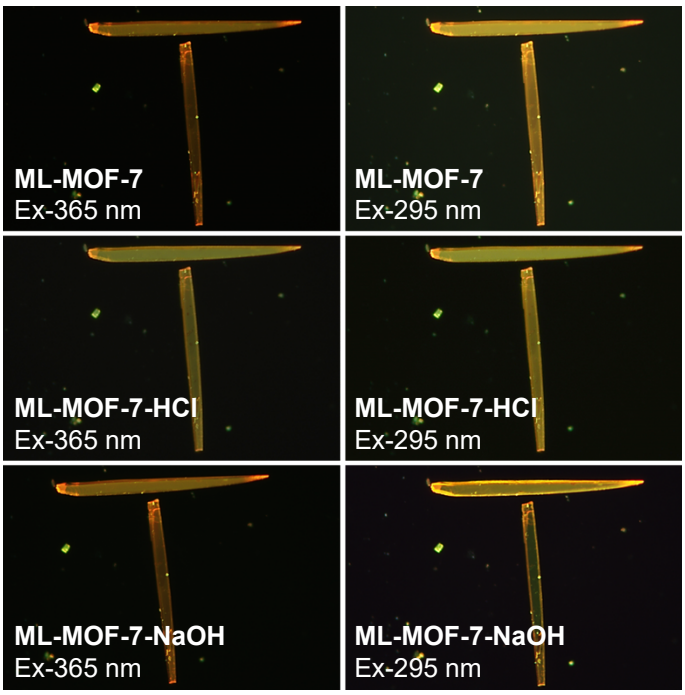

Figure S18. PL images of 'T' microcrystals made of **ML-MOF-7** under the excitation of 295 and 365 nm.

Initial **ML-MOF-7** microcrystals show orange-red emission (Ex-365 nm) and yellow emission (Ex-295 nm). After fuming of HCl, the microcrystals exhibit green emission under the of 295 nm and 365 nm UV lamps. Finally, the Ex-De behaviour recovered through the treatment of NaOH aqueous.

Operation details: Here, the **ML-MOF-7** were prepared via a stepwise hydrothermal method in a 10 mL glass vial. Then, the **ML-MOF-7** crystals were dropcast on the glass substrate (22*22 mm). In the HCl fumigation process, the glass substrate with **ML-MOF-7** crystals was turned upside down over a vial of HCl (8 M) at room temperature about 30 s. Then, the **ML-MOF-7-HCl** crystals were successfully prepared. Subsequently, the NaOH aqueous (2 M, 100 μL) was added to the **ML-MOF-7-HCl** crystals on the same glass substrate to obtain the **ML-MOF-7-NaOH** crystals.

Table S1. Crystal data and structure refinement for the **FJU-221** (CCDC No. 2288758).

Identification code	**FJU-221**
Empirical formula	$C_{46}H_{38}N_6O_{10}S_2Sr_2$
Formula weight	1074.18
Temperature/K	100.00(10)
Crystal system	triclinic
Space group	P-1
a/Å	8.99150(10)
b/Å	15.1440(2)
c/Å	18.4951(2)
α/°	108.4940(10)
β/°	99.8990(10)
γ/°	105.5790(10)
Volume/Å^3	2207.62(5)
Z	2
ρcalcg/cm^3	1.616
μ/mm^{-1}	4.637
F(000)	1088
Radiation	CuKα (λ = 1.54184)
2Θ range for data collection/°	5.25 to 155.902
Index ranges	-8 ≤ h ≤ 11, -18 ≤ k ≤ 19, -23 ≤ l ≤ 23
Reflections collected	43824
Independent reflections	9295 [Rint = 0.0644, Rsigma = 0.0519]
Data/restraints/parameters	9295/0/600
Goodness-of-fit on F^2	1.068
Final R indexes [I>=2σ (I)]	R1 = 0.0417, wR2 = 0.1147
Final R indexes [all data]	R1 = 0.0460, wR2 = 0.1185
Largest diff. peak/hole / e Å^{-3}	0.91/-1.24

Table S2. Photophysical parameters of the BTDB and the **ML-MOFs**.

	BTDB	ML-MOF-1	ML-MOF-2	ML-MOF-3	ML-MOF-4	ML-MOF-5	ML-MOF-6	ML-MOF-7	ML-MOF-8
QY	42.85	8.57	7.38	5.5	4.68	4.83	2.86	2.83	2.09
LifeTime/520nm	5.67	4.86	1.16	1.17	1.13	1.1	0.96	0.99	0.86
ET efficiency		14%	80%	79.4%	80%	81%	83%	83%	85%

The ET efficiency can be evaluated by the equation: $E = 1 - \tau_{da}/\tau_{d}$, where τ_{da} and τ_{d} is the excited-state lifetimes of donor in the presence and absence of the acceptor respectively[2].

References

1. H.-L. Xia, K. Zhou, S. Wu, D. Ren, K. Xing, J. Guo, X. Wang, X.-Y. Liu and J. Li, Building an emission library of donor–acceptor–donor type linker-based luminescent metal–organic frameworks, *Chem. Sci.*, 2022, **13**, 8036-8044.
2. H. Q. Zheng, Y. Yang, Z. Wang, D. Yang, G. Qian and Y. Cui, Photo-Stimuli-Responsive Dual-Emitting Luminescence of a Spiropyran-Encapsulating Metal–Organic Framework for Dynamic Information Encryption, *Adv. Mater.*, 2023, **35**, e2300177.